PI103 affects the progression of hepatic fibrosis through Ca 2+ and PI3K/Akt-dependent HSC apoptosis

Yu. Yan
North China University of Science and Technology
Haiying. Liu
North China University of Science and Technology
Linyu Dai
North China University of Science and Technology
Qian Xiao
North China University of Science and Technology
Yonghong Xiao (kycxyh@tom.com)
North China University of Science and Technology

Research Article

Keywords: PI103, PI3K/Akt, Apoptosis, Hepatic stellate cells, Hepatic fibrosis, Calcium

Posted Date: April 11th, 2022

DOI: https://doi.org/10.21203/rs.3.rs-1530570/v1

Abstract

Activated hepatic stellate cell (HSC) is the central link to the occurrence and development of liver fibrosis, which can be reversed by promoting the apoptosis of HSC. The activation of HSC leads to an increase in proliferation, collagen synthesis and the contraction of HSCs. The studies in vitro and in vivo have shown that intracellular Ca^{2+} plays an important role in the mediating apoptosis and contraction of HSC. The phosphatidyl inositol 3-kinase (PI3K)/Akt signalling pathway is closely related to the occurrence and development of liver fibrosis. In this study, we investigated the effect of PI3K inhibitor PI103 on HSC stimulated by transforming growth factor-β1(TGF-β1) and explored its relevant mechanisms. The results showed PI3K inhibitor PI103 could inhibit the proliferation of activated HSC, increase its apoptosis, decrease intracellular Ca^{2+} concentration and reduce the expression of signal molecules PI3K and Akt and type I, III collagen as well. Our study demonstrates that Ca^{2+} and PI3K/Akt-dependent HSC apoptosis may serve as a potential novel target for anti-fibrosis therapy.

Introduction

Hepatic fibrosis is a major cause of morbidity and mortality worldwide. The pathological process of hepatic fibrosis is an excessive proliferation of collagen based extracellular matrix, which is mainly type I and III collagen, when it reacts to a variety of chronic stimuli, and is deposited in the liver [1]. Liver fibrosis is the outcome of various chronic liver diseases and the only way of cirrhosis, and difficult to reverse once it develops into cirrhosis [2], so the treatment of liver fibrosis is particularly important. Because of the complexity of the molecular pathogenesis of liver fibrosis, there are few reports about the molecular mechanism of anti-hepatic fibrosis studied systematically and deeply around the cellular signal transduction pathway. Hepatic Stellate Cell (HSC) is the main source of extracellular matrix in hepatic fibrosis, and its activation and proliferation is the key to the formation of hepatic fibrosis [3, 4].

Studies have shown that Ca^{2+} play an important role in mediating HSC diastolic and apoptosis [5, 6]. The phosphatidyl inositol 3-kinase (PI3K) pathway is a signalling pathway activated by platelet-derived growth factor (PDGF)[7], the PI3K/Akt (protein kinase B) signaling pathway is widely involved in cell mitosis, cell differentiation, cell survival and migration [8], and is closely related to the occurrence and development of hepatic fibrosis[9, 10]. However, the influence of blocking PI3K/Akt signaling pathway on the hepatic fibrosis is not well understood. In addition, the precise mechanisms of PI3K/Akt pathway inhibitors in hepatic fibrosis remain largely unknown. PI103 is a PI3K inhibitor and its chemical formula is $C_{19}H_{16}N_4O_3$. Previous research has showed PI3K-mediated signaling blocked by PI103 has a profound effect on cellular proliferation in Glioblastoma multiforme cell lines [11]. Furthermore, PI3K inhibitors have exhibited favorable preclinical results [12].

In this experiment, PI3K inhibitor (PI103) was used to treat HSC stimulated by fibrogenic factor-transforming growth factor beta1 (TGF-β1) in vitro, the effects of PI103 on the PI3K/Akt signal pathway was examined and the possible therapeutic effect of PI3K inhibitor was investigated, and the apoptosis

rate and the intracellular Ca^{2+} concentration changes were observed to provide a theoretical basis for the treatment of hepatic fibrosis.

Materials And Methods

Cell culture Hepatic stellate cell lines cirrhotic fat storing cell (CFSC) isolated from carbon tetrachloride (CCl_4)- induced cirrhosis rats and acquired permanent natural properties were built and presented by professor Greenwel [13] of the United States. The cells frozen in liquid nitrogen were resuscitated and inoculated in Dulbecco's modified Eagle's medium (DMEM) (Boehringer Ingelheim Corporation, USA) containing 5% fetal bovine serum (FBS) (Hangzhou Sijiqing Biological Products Company, China) and 1% penicillin streptomycin mixed solution in humidified air at 37℃ with 5% CO_2. When the cells were monolayer dense, they were digested by 0.25% trypsin and passaged.

Cell grouping and treatment The cells were synchronized for 24h, then divided into three groups: control group, TGF-β1 group, TGF-β1 + PI103 (Selleck Chemicals, USA) group. The control group was grown in complete medium for 48h, the TGF-β1 group was grown in complete medium with 5ng/mL TGF-β1 for 48h, and TGF-β1 + PI103 group was grown in complete medium with 5ng/mL TGF-β1 for 24h, then 4μmol/L PI103 was added for 24h. In addition, HSCs were treated in a dose-dependent manner by PI103 to observe the effect of PI103 on HSCs proliferation.

Cell proliferation assay HSCs proliferation of each group was determined by MTT (3–4,5-Dimethylthiazol-2-yl-2,5-diphenyltetrazolium bromide). The cell suspension was seeded in 96-well plates at a density of 2×10^4 cells/mL and 200μl per well. Each group was comprised of five wells and an empty zero well, 20μL of 5g/L MTT (Sigma Company, USA), was added for 4h in each well and 200μL DMSO (Dimethyl sulfoxide) (Sigma Company, USA) was added, then cells were exposed to a miniature oscillator shock for 10min. The enzyme-labelled instrument was set to deliver a single wave excitation at 490nm to measure the cell absorbance value (A). The cell proliferation rate (PR) was calculated. PR = T/C×100%, where T is the A value of the treatment group and C is the A value of the control group.

Cell morphological changes assay Morphological changes of the cells were observed under transmission electron microscopy (HITACHI Company, Japan). The cells in the control group, TGF-β1 group and TGF-β1 + PI103 group were centrifuged and fixed. After dehydration, transparency, waxing, embedding, slicing and staining, the cellular internal structure was observed under transmission electron microscopy.

HSC apoptosis detection The cells in each group were digested, centrifuged and collected, and washed with cold PBS(phosphate buffer saline), 1xBinding buffer 195μL and 5μL Annexin V (MultiSciences Lianke Biotechnology Corporate Limited) were added into the cells, mixed gently for 30 min, centrifuged and precipitated, discarded the supernatant, then added in 1x Binding buffer 195μL and 5μL PI (Propidine iodide) (MultiSciences Lianke Biotechnology Corporate Limited), blow and mixed gently. The apoptosis of cells was examined with Flow cytometry (Becton, Dickinson Company).

Observation of Ca $^{2+}$ concentration The loaded cells were rinsed 2–3 times with PBS, and incubated at 37˚C, 5% CO_2 for 20 min after adding 1mL DMEM (Boehringer Ingelheim Corporation), then was observed with a laser scanning confocal microscope (Olympus Corporation, Japan). The Fluo-3-Acetoxymethyl ester (Fluo-3AM) excitation wavelength was 488 nm and the emission wavelength was 530 nm, Ca^{2+} fluorescence absorbance was scanned. The average fluorescence intensity of the whole cell was calculated by the data from the laser scanning confocal microscope and the image processing software FV10-ASW1.7 Viewer. The relative value of fluorescence intensity was recorded in the experiment to observe the dynamic change of the Ca^{2+}concentration. The fluorescence intensity changes when the concentration of Ca^{2+} changes in the HSCs loaded with Fluo-3AM. The change of Ca^{2+} concentration is indicated by fluorescence intensity, and the higher the fluorescence intensity, the higher the concentration of Ca^{2+}. Therefore, the fluorescence intensity of each cell was measured to indicate the intracellular Ca^{2+} concentration. In each group, 6 HSCs were randomly selected, scanned for fluorescence, and the average intensity value was calculated.

RT-qPCR assay Total RNA was extracted from HSCs using RNA extraction kit (Invitrogen, Thermo Fisher Scientific, Inc., Rockford, IL, USA) following the manufacturer's instructions. The extracted RNA was reverse transcribed using M-MLV Reverse Transcriptase (Thermo Fisher Scientific, Inc.). Subsequently, real-time fluorescence quantitative polymerase chain reaction PCR(RT-qPCR) was performed with SYBR-Green PCR kit (Thermo Fisher Scientific, Inc.) according to manufacturer's instructions. The following primers were used for qPCR: PI3K, forward 5’ TAG GCT CCA AAC CGT TCT TTA TG3’ and reverse 5’ GAT GAC GAG GAT TTG CTG ATG TA3’; Akt, forward 5’GCT GAG TAG GAG AAC TGG GGA AA 3’ and reverse 5’ TGA GAC CGA CAC CAG GTA TTT TG 3’. RT-qPCR was performed with 2μg total RNA and the target genes PI3K and Akt were simultaneously amplified using the above 50μL reaction system. Specific cycle parameters were as follows: RT: 41 ℃ 45 min; PCR: 95 ℃ pre-denaturation 10 min into the cycle, 95 ℃ denaturation 15sec, 60 ℃ annealing 1min, 72 ℃ extension 1.5min, 35 cycles after 72 ℃ extension 10min. Calculation of mRNA expression of target gene. In RT-qPCR, each sample was repeated three times, taking the mean value as Ct value. The Ct value is the cycle number of the fluorescence threshold in the heat cycle instrument. The fluorescence quantitative analysis was performed with the PCR amplification instrument and the $\triangle$Ct value was calculated. Relative quantitative $2^{-\Delta\Delta Ct}$ method was used to compare the difference of target gene mRNA expression.

Immunohistochemistry assay Immunofluorescence staining was performed using the streptomycin biotin-peroxidase immunohistochemistry kit (SP method) (Beijing Zhongshan Jinqiao company, China), the experimental procedure was performed according to the kit instructions, the primary antibody concentration (PI3K, Akt antibody-Beijing Biosynthesis Biotechnology, China; Type I, III collagen antibody-Wuhan Boster Biological Technology, China) was 1: 100, and PBS instead of primary antibodies was used as a negative control. The positive expression of protein was a diffuse brown yellow staining in the cytoplasm. The stained cells were observed under microscope. The optical density of images was detected by Image-Pro Plus software, the average optical density of each slice was randomly taken from

6 visual fields at a magnification, x200 as the expression of PI3K, Akt signal molecule and type I, III collagen.

Western blot assay After HSCs were treated with TGF-β1 and PI103, the total cell proteins were extracted with RIPA(Radio immunoprecipitation assay) lysis buffer (Wuhan Bobst Biotechnology Co., Ltd., China). After 30 min of complete lysis, the cells were centrifuged at 12000 r/min at 4℃ for 20 min. Protein concentration was determined using BCA Protein Detection Kit (Solarbio Science & Technology Co., Ltd., Beijing, China). Protein loading system was 20μg/10μl/well. Electrophoresis was performed on 10% SDS-PAGE (sodium dodecyl sulfate-polyacrylamide gel electrohoresis) gel preparation kit (Zoman Biotechnology Co., Ltd., Beijing, China), and electrically transferred to 0.45 μm PVDF(Polyvinylidene fluoride) membrane. PVDF membrane was sealed with 5% skim milk for 2 h at room temperature, then incubated with primary antibody (anti-phosphorylated-Akt (p-Akt) antibody: 1:1500; #bsm-52130R; Bioss Biological Co. Ltd., Beijing, China; anti-cleaved-caspase 3 antibody: 1:1500; #AF7022; Affinity Biosciences. Co. Ltd., USA; anti-caspase 3 antibody: 1:1500; #AF6311; Affinity Biosciences. Co. Ltd., USA.) at 4℃ overnight, washed with TBST(Tris-buffered saline Tween) for 3 times, and incubated with horseradish peroxidase-conjugated anti-rabbit (1:5000; # ZB2307, Zsbio Commerce Store, Beijing, China) secondary antibody at room temperature for 1 h. Protein bands were detected using an ECL luminescent reagent kit (Pierce Biotechnology, Inc., USA) and Image J software (version 1.6.0; National Institutes of Health) analysis of protein gray values.

Statistical Analysis The obtained data were processed by SPSS 20.0 statistical analysis software. Results were described as means ± SD ($\bar{x} \pm s$). The multiple groups were compared with a one-way analysis of variance (ANOVA), and the minimum difference significant method (LSD) was used for pairwise comparison. The difference in $P < 0.05$ was statistically significant.

Results

Effect of PI3K inhibitor PI103 on proliferation The PR value of HSC in TGF-β1 group was significantly increased compared with the control group ($P < 0.05$). TGF-β1 + 1μmol/LPI103 group, TGF-β1 + 2μmol/LPI103 group, TGF-β1 + 4μmol/LPI103 group HSC PR value was less than that of TGF-β1 group ($P < 0.05$). With the increase of PI103 dose, HSC PR value decreased. The HSC PR value of TGF-β1 + 4μmol/LPI103 group was similar to that of TGF-β1 + 2μmol/LPI103 group ($P > 0.05$) (Fig. 1A).

There were significant differences in the PR value among groups ($F = 67.67$, $P < 0.05$). Compared with the control group, the PR value in the TGF-β1 group increased significantly ($P < 0.05$). The PR value in TGF-β1 + PI103(4μmol/L) group was significantly lower than that in the TGF-β1 group($P < 0.05$) (Fig. 1B).

Morphological changes of the cells were observed under transmission electron microscopy

In the control group, the cells were irregular in morphology, and there were branched pseudo feet on the periphery, abundant cytoplasm, lipid droplets, mitochondria, and endoplasmic reticulum. Mitotic cells were occasionally visible and apoptotic cells were rarely seen (Fig. 2A). In the TGF-β1 group, the number of cells increased at the mitotic stage, the cytoplasm was more abundant, the lipid droplets decreased, the mitochondria and the endoplasmic reticulum increased, the small amount of collagen fibrous cells were found between cells, and apoptotic cells were rare (Fig. 2B). In the TGF-β1 + PI103 group, the number of apoptotic cells increased, characterized by nuclear pyknosis, an increased proportion of nucleus to cytoplasm, less cytoplasm, mitochondria disintegrating into vacuoles or swelling, chromatin condensation and concentration along the nuclear membrane with distinct flower petal mass or crescent shape. Occasionally, nucleus fragmentation and apoptotic body were seen (Fig. 2C).

Effect of PI3K inhibitor PI103 on apoptosis Apoptosis of HSC in different treatment groups was detected by flow cytometry (Fig. 3A). There was significance difference in apoptosis rate among groups (F = 115.00, P < 0.05). The apoptosis rates in the control group and TGF-β1 group were (1.70 ± 0.17)% and (2.97 ± 0.28)% respectively, and there was no significant difference between two groups (P > 0.05), while which in TGF-β1 + PI103 group (10.30 ± 0.68) % was significantly higher than those in the control group and the TGF-β1 group, the difference was statistically significant (P < 0.05) (Fig. 3B).

Effect of PI3K inhibitor PI103 on Ca^{2+}

The fluorescence intensity of cells in each group was different (Fig. 4). There were significant differences in Ca^{2+} concentration among groups (F = 16.36, P < 0.05). The intracellular Ca^{2+} concentration in the TGF-β1 group was higher than that in the control group, while which in TGF-β1 + PI103 group was between the control group and TGF-β1 group. The intracellular Ca^{2+} concentration of HSC in the control group, TGF-β1 group and TGF-β1 + PI103 group was (1037.82 ± 65.99), (1697.28 ± 212.14) and (1379.11 ± 265.22) respectively, and the difference was statistically significant between pairwise comparison (P < 0.05) (Fig. 4).

Expressions of mRNA of PI3K and Akt signal molecules The mRNA expression of PI3K signal molecule in the control group was set to 1, and the expression multiple of PI3K signal molecule in the TGF-β1 group and TGF-β1 + PI103 group was 1.84 and 0.77 respectively. Compared with the control group, the PI3K mRNA expression in the TGF-β1 group was significantly increased, while which in TGF-β1 + PI103 group was significantly decreased, and the difference was statistically significant (P < 0.05). The mRNA expression of PI3K signal molecule in TGF-β1 + PI103 group was decreased when compared with the TGF-β1 group (P < 0.05). The expression multiple of Akt signal molecule mRNA in the control group was set to 1; The mRNA expression of Akt signal molecules in the TGF-β1 group and TGF-β1 + PI103 group were 1.72 and 0.87 respectively. Compared with the control group, the Akt mRNA expression of TGF-β1 groups significantly increased (P < 0.05), and the expression of TGF-β1 + PI103 group was slightly reduced, and the difference was not statistically significant (P > 0.05). Comparison of TGF-β1 + PI103 group and TGF-β1 group, the expression of Akt signal molecule mRNA significantly decreased (P < 0.05) (Fig. 5).

Protein expressions of PI3K, Akt and type Ⅰ, III collagen The results of immunocytochemistry showed that the positive expressions of PI3K, Akt signal molecule and type I, III collagen were all brown-yellow granules deposited in the cytoplasm of hepatic stellate cells, which were found in all groups and there was obvious around the nucleus, but the number of positive cells and the depth of staining were different in each group. Compared with the blank control group, the number of positive cells in TGF-β1 group was more and the color was deepened. After adding PI3K inhibitor PI103, the number of positive cells decreased and the staining became lighter(Fig. 6A).

Image analysis showed that the expressions of PI3K, Akt signal molecule and type Ⅰ, III collagen in TGF-β1 group were increased when compared with the control group, and the differences were statistically significant ($P < 0.05$), while compared with TGF-β1 group, which in TGF-β1 + PI103 group decreased, and the difference were statistically significant ($P < 0.05$)(Fig. 6B).

The protein expressions of p-Akt, caspase-3 and cleaved caspase-3 The protein expressions of p-Akt, caspase-3 and cleaved caspase-3 were detected by western blot (Fig. 7A and B). The protein expression of p-Akt and cleaved caspase-3 in the TGF-β1 group increased significantly, while which of caspase-3 decreased when compared with the control group ($P < 0.05$). Compared with the TGF-β1 group, the protein expression of p-Akt in TGF-β1 + PI103 group decreased ($P < 0.05$), while which of caspase-3 and cleaved caspase-3 in TGF-β1 + PI103 group increased significantly ($P < 0.05$).

Discussion

The occurrence of liver fibrosis is the result of the formation and degradation of the interstitial fibres of liver cells, while the activated HSC is the main source of the extracellular matrix. The activation and proliferation of HSCs is the central event in the occurrence of liver fibrosis [14]. Promoting the apoptosis of HSCs, reducing the number of HSCs and reducing the extracellular matrix have become new strategies for the treatment of liver fibrosis [15, 16]. PI103 is a powerful compound that inhibits the activity of enzymes related to growth and proliferation at low concentrations and reduces the degree of phosphorylation of PKB/Akt by inhibiting PI3K, thus inducing cell cycle stagnation in the G_0/G_1 phase [17]. There are many researches about PI103 inhibiting proliferation and promoting apoptosis of tumor cells, however, PI103 has not been reported in HSC research.

In this experiment, the proliferation rate of cells in TGF-β1 group was 2.72 times higher than that in control group, while which in HSC stimulated by TGF-β1 was reduced by 4μmol/L PI103, and 4μmol/L PI103 increased the apoptosis rate of HSC ($P < 0.05$). These results indicated that TGF-β1 could significantly promote the proliferation of HSC, PI3K inhibitor PI103 could significantly inhibit the proliferation and promote the apoptosis of HSC. Transmission electron microscopy also confirmed that there were typical characteristics of apoptosis in TGF-β1 + PI103 group.

Studies have shown that the activation of PI3K made Akt transposition to the cell membrane, activated the Akt completely and changed conformation [18], then the activated Akt could transfer anti-apoptotic

signal to its downstream channel effect factor, thus played the role of antagonism to cell apoptosis and promoted cell growth and proliferation. Activation of PI3K/Akt pathway in hepatic stellate cells promotes hepatic fibrosis [19]. PI103, an inhibitor of PI3K, mould inhibit the HSC proliferation and promote the HSC apoptosis through negative regulation of PI3K signalling pathway.

During the activation of HSC, calcium channels in HSC were opened to a great extent, which caused significant cell contraction. The increase of Ca^{2+} concentration in HSC is directly related to the contraction of HSCs [20]. In the experiment, the effect of TGF-β1 and PI103 on the Ca^{2+}concentration was observed by laser scanning confocal microscopy (LSCM) using a calcium fluorescence probe Fluo-3AM. When compared with the control group, the fluorescence intensity of HSC in TGF-β1 group enhanced, Ca^{2+} concentration increased, and the difference was statistically significant ($P < 0.05$). TGF-β1 could cause calcium overload in HSCs. The mechanism of Ca^{2+} elevation in HSC induced by TGF-β1 mould be related to the change of activity and gene expression level of Na^{+}/Ca^{2+} exchanger [21]. After the PI3K inhibitor PI103 was used to treat the HSC stimulated by TGF-β1, the Ca^{2+} fluorescence intensity weakened, Ca^{2+} concentration decreased, and the difference was statistically significant ($P < 0.05$) when compared with the TGF-β1 group. PI103 mould inhibit the contraction and promote apoptosis of HSC possibly by reducing the concentration of Ca^{2+}, but the specific mechanism of action was unknown, and further study was needed.

The results of RT-qPCR showed that the mRNA level of PI3K and Akt was higher in TGF-β1 group than that in the control group ($P < 0.05$), which in TGF-β1 + PI103 group decreased ($P < 0.05$) when compared with TGF-β1 group, and it indicated that PI3K inhibitor PI103 inhibited the gene expression of PI3K and its downstream signaling molecule Akt. The results of immunocytochemistry showed that the expressions of type I and III collagen were increased in hepatic stellate cells stimulated by TGF-β1 in vitro, PI3K inhibitor PI103 could reduce the expression of type I and III collagen, and the difference was statistically significant ($P < 0.05$). It suggested that PI103 could block the process of hepatic fibrosis by inhibiting the expression of type I and III collagen in hepatic stellate cell. The research has reported that Tormentic acid promoted cell apoptosis and inhibited the expression of collagen type I and III, and inhibited the phosphorylation of PI3K and Akt via the inhibition of the PI3K/Akt pathway [22]. Another study has showed that blocking PI3K/Akt pathway led to inhibit HSC activation [23].

Caspase-3 is the most important protease in the process of apoptosis, the most critical executor of apoptosis in the downstream of caspase, and plays the final pivotal role in the apoptosis process initiated by various factors[24]. Caspase-3 usually exists in the cytoplasm in the form of zymogen, which is activated in the early stage of apoptosis, and cleaved caspase-3 is an activated form of caspase-3[25]. In this study, the results of Western blot showed that PI103 increased the protein expression of caspase-3 and cleaved caspase-3, these suggested that PI103 increased the expression of caspase-3, an apoptotic protein, and promoted the apoptosis of HSC. The intervention of PI103 may bring new hints for anti-fibrosis therapy.

Conclusion

PI3K/Akt pathway is an important signal transduction pathway in cells, which can promote the proliferation of HSCs. PI3K inhibitor PI103 could promote apoptosis of HSCs, inhibit the cell proliferation, decrease the intracellular Ca^{2+} concentration, reduce the phosphorylation of Akt, block the conduction of PI3K/Akt signaling pathway, increase the protein expression of caspase-3 and cleaved caspase-3,thereby reduce the formation of type I and III collagen, and these provided the theoretical basis for the treatment of hepatic fibrosis. Our study demonstrates that PI3K inhibitor PI103 can restrain the progression of hepatic fibrosis through PI3K/Akt-dependent HSC apoptosis, and which may serve as a potential novel target for anti-fibrosis therapy.

Declarations

Funding This study was supported by a grant (H2015209043)from Natural Science Foundation of Hebei Province.

Conflict of interest The authors declare no conficts of interest.

Author contributions YY and YX wrote the main manuscript text. HL and LD performed experiments. QX analyzed data and prepared figures. All authors read and approved the final manuscript.

Data availability All the data generated or analyzed during this study have been included in this article.

Ethics approval This study does not involve human participants and/or animals, and no ethical approval is required.

Informed consent All the authors meet the qualifcations for authorship and had an opportunity to read and comment the manuscript. All authors support publication of the manuscript in Molecular and Cellular Biochemistry.

References

1. Parola M, Pinzani M (2019) Liver fibrosis: Pathophysiology, pathogenetic targets and clinical issues. Mol Aspects Med 65:37–55. https://doi.org/ 10.1016/j.mam.2018.09.002
2. Caballeria L, Pera G, Arteaga I, Rodríguez L, Alumà A, Morillas RM, de la Ossa N, Díaz A, Expósito C, Miranda D, Sánchez C, Prats RM, Urquizu M, Salgado A, Alemany M, Martinez A, Majeed I, Fabrellas N, Graupera I, Planas R, Ojanguren I, Serra M, Torán P, Caballería J, Ginès P(2018) High prevalence of liver fibrosis among European adults with unknown liver disease: a population-based study. Clin Gastroenterol Hepatol 16:1138–1145.e5. https://doi.org/10.1016/j.cgh.2017.12.048
3. El-Mezayen NS, El-Hadidy WF, El-Refaie WM, Shalaby TI, Khattab MM, El-Khatib AS (2017) Hepatic stellate cell-targeted imatinib nanomedicine versus conventional imatinib: A novel strategy with

potent efficacy in experimental liver fibrosis. J Control Release 266:226–237. https://doi.org/10.1016/j.jconrel.2017.09.035

4. Zisser A, Ipsen DH, Tveden-Nyborg P (2021) Hepatic stellate cell activation and inactivation in NASH-fibrosis-roles as putative treatment targets. Biomedicines 9:365. https://doi.org/10.3390/biomedicines9040365
5. Laleman W, Van Landeghem L, Severi T, Vander Elst I, Zeegers M, Bisschops R, Van Pelt J, Roskams T, Cassiman D, Fevery J, Nevens F (2007) Both Ca2+ -dependent and -independent pathways are involved in rat hepatic stellate cell contraction and intrahepatic hyperresponsiveness to methoxamine. Am J Physiol Gastrointest Liver Physiol 292: G556-564. https://doi.org/10.1152/ajpgi.00196.2006
6. Liu H, Wang L, Dai L, Feng F, Xiao Y (2021) CaMK II/Ca2 + dependent endoplasmic reticulum stress mediates apoptosis of hepatic stellate cells stimulated by transforming growth factor beta 1. Int J Biol Macromol 172:321–329. https://doi.org/10.1016/j.ijbiomac.2021.01.071
7. Du Z, Lin Z, Wang Z, Liu D, Tian D, Xia L (2020) SPOCK1 overexpression induced by platelet-derived growth factor-BB promotes hepatic stellate cell activation and liver fibrosis through the integrin α5β1/PI3K/Akt signaling pathway. Lab Invest. 100:1042–1056. https://doi.org/10.1038/s41374-020-0425-4
8. Kao YH, Chen PH, Wu TY, Lin YC, Tsai MS, Lee PH, Tai TS, Chang HR, Sun CK (2017) Lipopolysaccharides induce Smad2 phosphorylation through PI3K/Akt and MAPK cascades in HSC-T6 hepatic stellate cells. Life Sci 184:37–46. https://doi.org/10.1016/j.lfs.2017.07.004
9. El-Mihi KA, Kenawy HI, El-Karef A, Elsherbiny NM, Eissa LA (2017) Naringin attenuates thioacetamide-induced liver fibrosis in rats through modulation of the PI3K/Akt pathway. Life Sci 187:50–57. https://doi.org/10.1016/j.lfs.2017.08.019
10. Zhu L, Cheng M, Liu Y, Yao Y, Zhu Z, Zhang B, Mou Q, Cheng Y (2017) Thymosin-beta4 inhibits proliferation and induces apoptosis of hepatic stellate cells through PI3K/AKT pathway. Oncotarget 8:68847–68853. https://doi.org/10.18632/oncotarget.18748
11. Ströbele S, Schneider M, Schneele L, Siegelin MD, Nonnenmacher L, Zhou S, Karpel-Massler G, Westhoff MA, Halatsch ME, Debatin KM (2015) A Potential Role for the Inhibition of PI3K Signaling in Glioblastoma Therapy. PLoS One 10:e0131670. https://doi.org/10.1371/journal.pone.0131670
12. Zhao HF, Wang J, Shao W, Wu CP, Chen ZP, To ST, Li WP (2017) Recent advances in the use of PI3K inhibitors for glioblastoma multiforme: current preclinical and clinical development. Mol Cancer 16:100–116. https://doi.org/10.1186/s12943-017-0670-3
13. Li Y, Yan Y, Liu F, Wang L, Feng F, Xiao Y (2018) Effects of calpain inhibitor on the apoptosis of hepatic stellate cells induced by calcium ionophore A23187. J Cell Biochem 119:1–9. https://doi.org/10.1002/jcb.27478
14. Jiang JX, Venugopal S, Serizawa N, Chen X, Scott F, Li Y, Adamson R, Devaraj S, Shah V, Gershwin ME, Friedman SL, Török NJ(2010) Reduced nicotinamide adenine dinucleotide phosphate oxidase 2

plays a key role in stellate cell activation and liver fibrogenesis in vivo. Gastroenterology 139:1375–1384. https://doi.org/10.1053/j.gastro.2010.05.074

15. Yang JH, Kim SC, Kim KM, Jang CH, Cho SS, Kim SJ, Ku SK, Cho IJ, Ki SH (2016) Isorhamnetin attenuates liver fibrosis by inhibiting TGF-β/Smad signaling and relieving oxidative stress. Eur J Pharmacol 783:92–102. https://doi.org/10.1016/j.ejphar.2016.04.042
16. Li G, Li D, Xie Q, Shi Y, Jiang S, Jin Y(2008) RNA interfering connective tissue growth factor prevents rat hepatic stellate cell activation and extracellular matrix production. J Gene Med 10:1039–1047. https://doi.org/10.1002/jgm.1223
17. Tsvetkov D, Shymanets A, Huang Y, Bucher K, Piekorz R, Hirsch E, Beer-Hammer S, Harteneck C, Gollasch M, Nürnberg B (2016) Better Understanding of Phosphoinositide 3-Kinase (PI3K) Pathways in Vasculature: Towards Precision Therapy Targeting Angiogenesis and Tumor Blood Supply. Biochemistry (Mosc) 81:691–699. https://doi.org/10.1134/S0006297916070051
18. Fresno Vara J, Casado E, de Castro J, Cejas P, Belda-Iniesta C, González-Barón M (2004) PI3K/Akt signalling pathway and cancer. Cancer Treat Rev 30:193–204. https://doi.org/10.1016/j.ctrv.2003.07.007
19. Cai CX, Buddha H, Castelino-Prabhu S, Zhang Z, Britton RS, Bacon BR, Neuschwander-Tetri BA (2017) Activation of Insulin-PI3K/Akt-p70S6K Pathway in Hepatic Stellate Cells Contributes to Fibrosis in Nonalcoholic Steatohepatitis. Dig Dis Sci 62:968–978. https://doi.org/10.1007/s10620-017-4470-9
20. Zhang XL, Xiao B, Meng Y, Li X (2011) Aldosterone stimulates hepatic stellate cells contraction via Ca2+-independent pathways. Chin J Hepatol 19:537–541. https://doi.org/10.3760/cma.j.issn.1007-3418.2011.07.016
21. Di Sario A, Svegliati Baroni G, Bendia E, Ridolfi F, Saccomanno S, Ugili L, Trozzi L, Marzioni M, Jezequel AM, Macarri G, Benedetti A (2001) Intracellular pH regulation and Na+/H + exchange activity in human hepatic stellate cells: effect of platelet-derived growth factor, insulin-like growth factor 1 and insulin. J Hepatol 34:378–385. https://doi.org/10.1016/s0168-8278(00)00062-3
22. Lin X, Li Y, Zhang X, Wen S, Lu Z, Huang Q, Wei J (2021) Tormentic acid inhibits hepatic stellate cells activation via blocking PI3K/Akt/mTOR and NF-κB signalling pathways. Cell Biochem Funct 39:77–87. https://doi.org/10.1002/cbf.3564
23. Fang B, Wen S, Li Y, Bai F, Wei Y, Xiong Y, Huang Q, Lin X (2021) Prediction and verification of target of helenalin against hepatic stellate cell activation based on miR-200a-mediated PI3K/Akt and NF-κB pathways. Int Immunopharmacol 92:107208. https://doi.org/10.1016/j.intimp.2020.107208
24. Nichani K, Li J, Suzuki M, Houston JP(2020) Evaluation of caspase-3 activity during apoptosis with fluorescence lifetime-based cytometry measurements and phasor analyses. Cytometry A 97:1265–1275. https://doi.org/10.1002/cyto.a.24207
25. Bernard A, Chevrier S, Beltjens F, Dosset M, Viltard E, Lagrange A, Derangère V, Oudot A, Ghiringhelli F, Collin B, Apetoh L, Feron O, Chen S, Arnould L, Végran F, Boidot R (2019) Cleaved caspase-3 transcriptionally regulates angiogenesis-promoting chemotherapy resistance. Cancer Res79:5958–5970. https://doi.org/10.1158/0008-5472.CAN-19-0840.

Figures

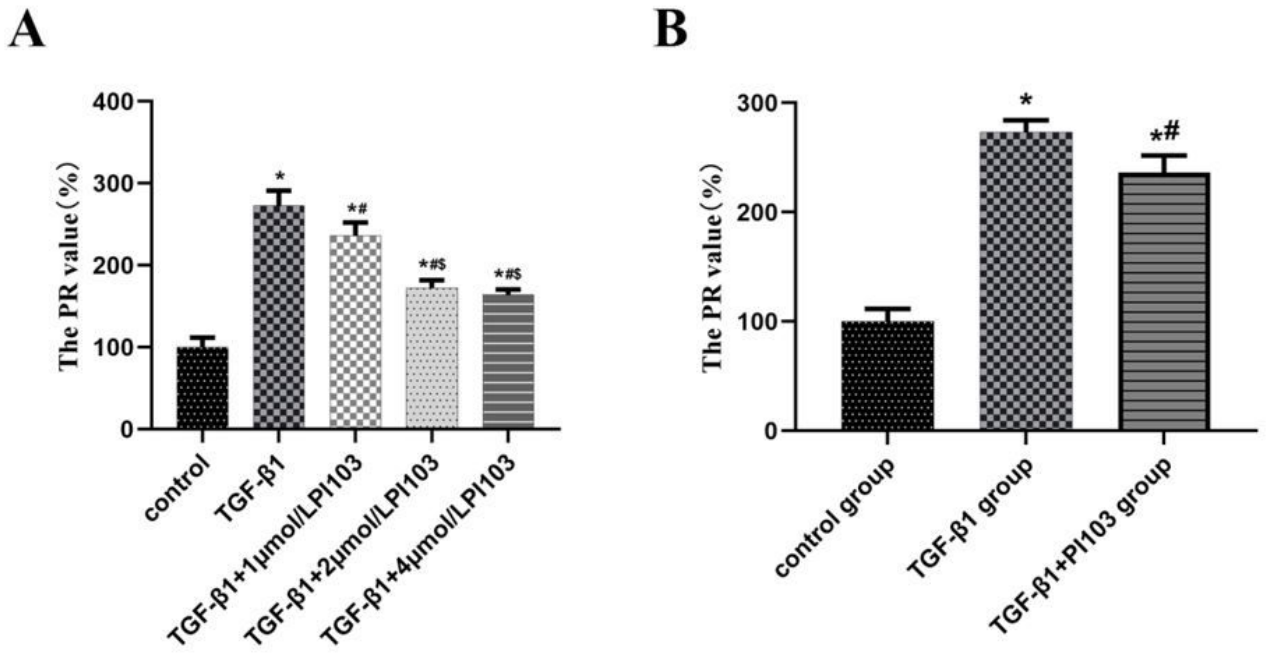

Figure 1

The proliferation rates (PR) of hepatic stellate cells in different groups. * P<0.05 compared with the control group; $^{\#}P$<0.05 compared with TGF-β1 group; $^{\$}$ P<0.05 compared with TGF-β1+1μmol/LPI103 group.

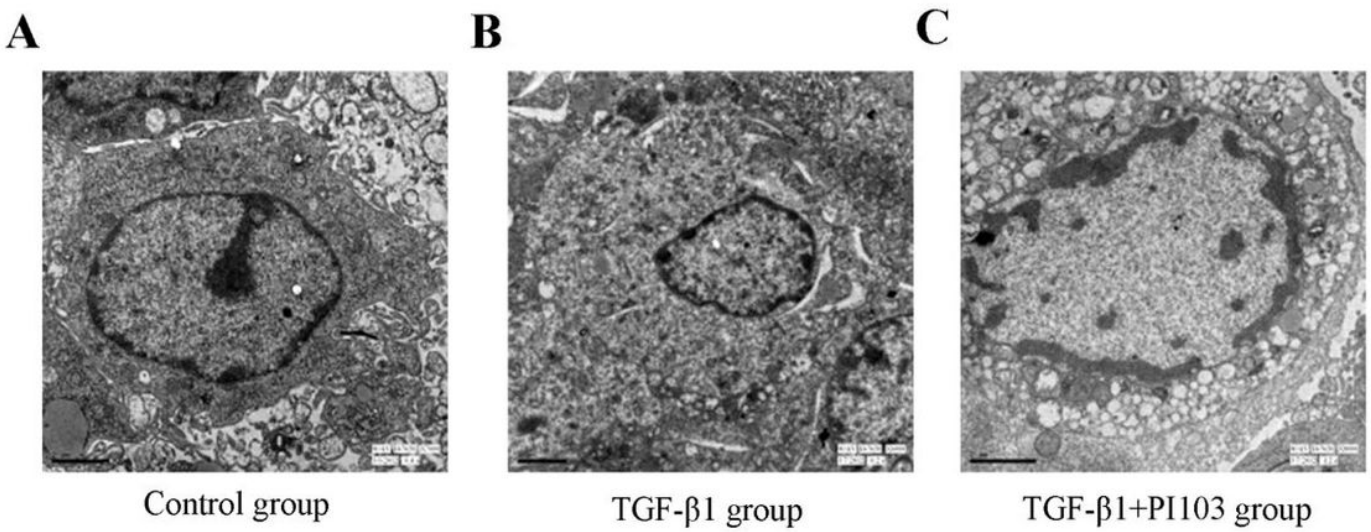

Figure 2

Morphological changes of hepatic stellate cells in different treatment groups. A: control group (×7000); B: TGF-β1 group (×6000); C: TGF-β1+ PI103 group (×8000).

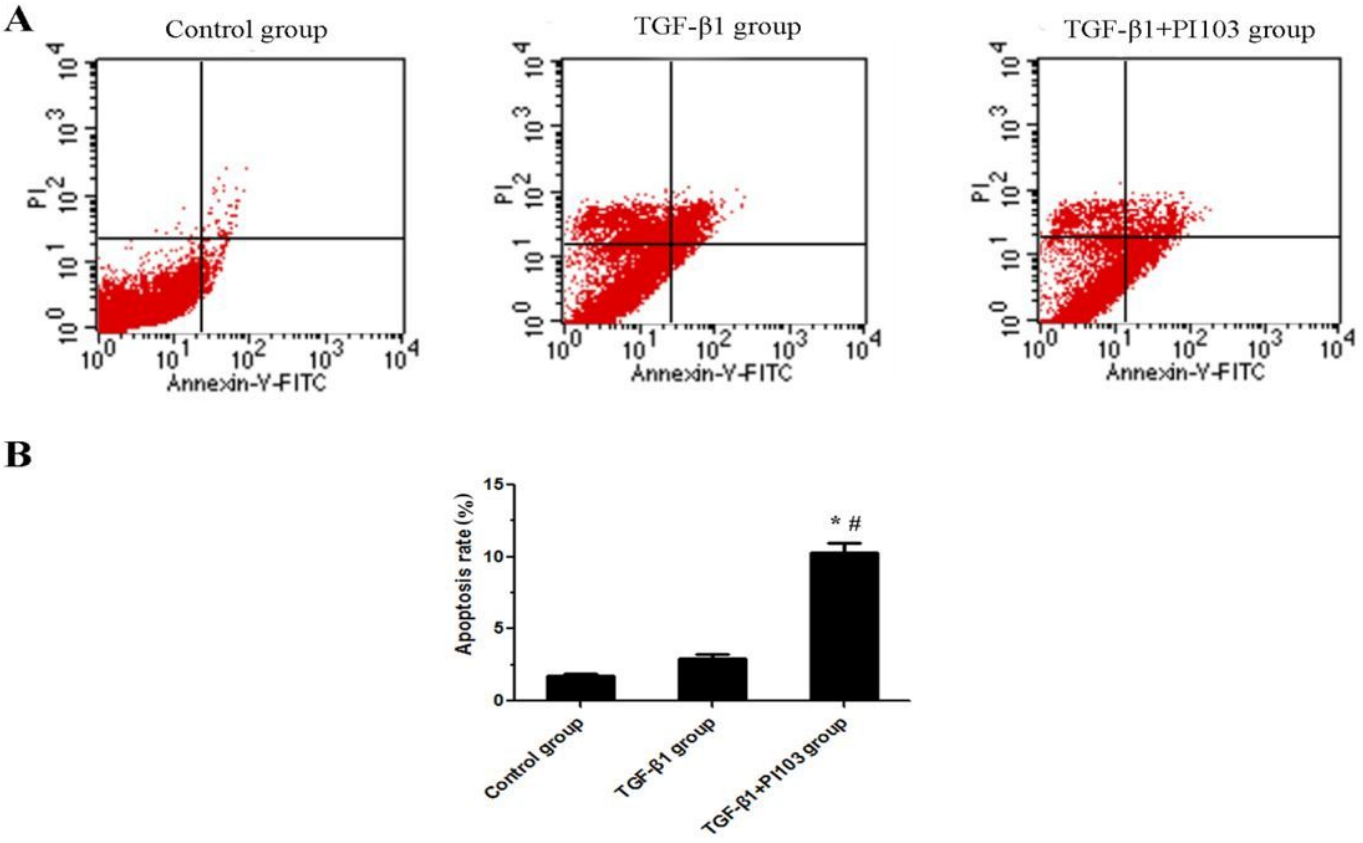

Figure 3

Apoptosis of hepatic stellate cells in different treatment groups detected by flow cytometry. **A** Apoptosis rates of HSC cells were detected by Annexin V-FITC/PI staining. **B** The percentages of apoptosis HSC cells after different treatment. * represents $P<0.05$ compared with the control group; # represents $P<0.05$ compared with TGF-β1 group.

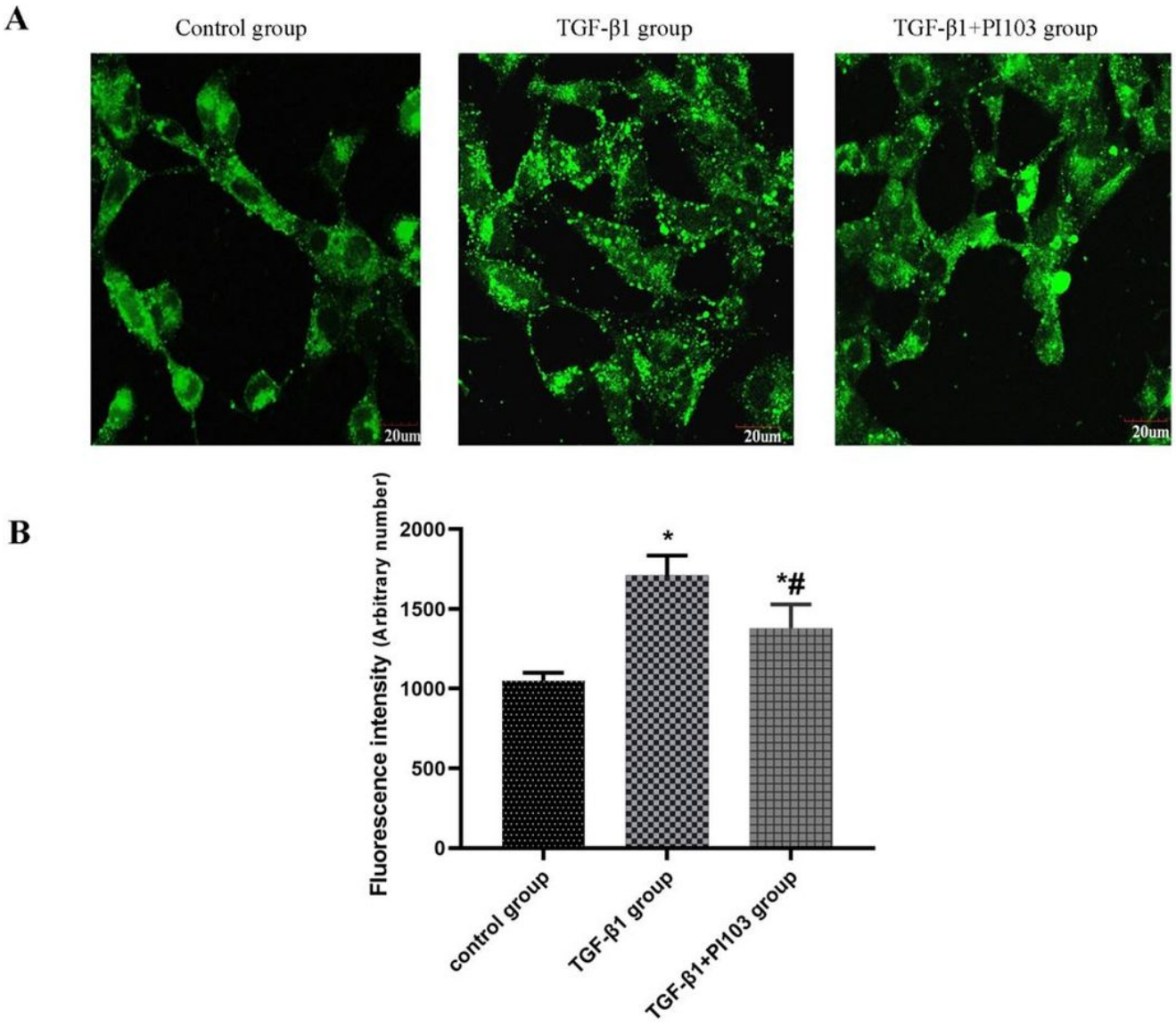

Figure 4

Ca^{2+} fluorescence intensity of hepatic stellate cells in different treatment groups detected by the laser confocal scanning microscope. **A** Ca^{2+} fluorescence intensity. **B** Intracellular Ca^{2+} concentration. * P<0.05 compared to the control group; $^{\#}$ P<0.05 compared with TGF-β1 group.

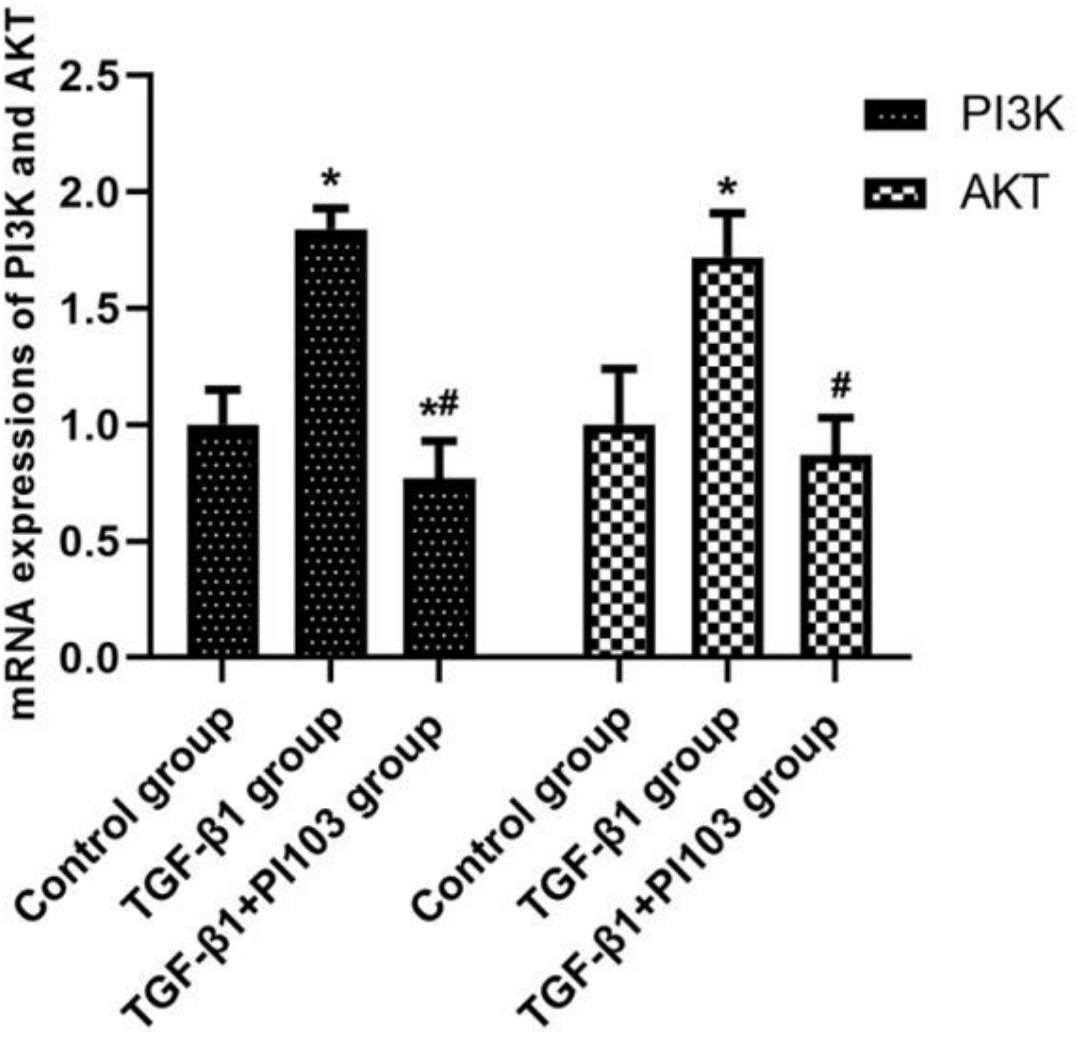

Figure 5

The relative multiple of mRNA expression of PI3K and Akt signal molecule in different groups. *P<0.05, when compared with the control group; #P<0.05, when compared with TGF-β1 group.

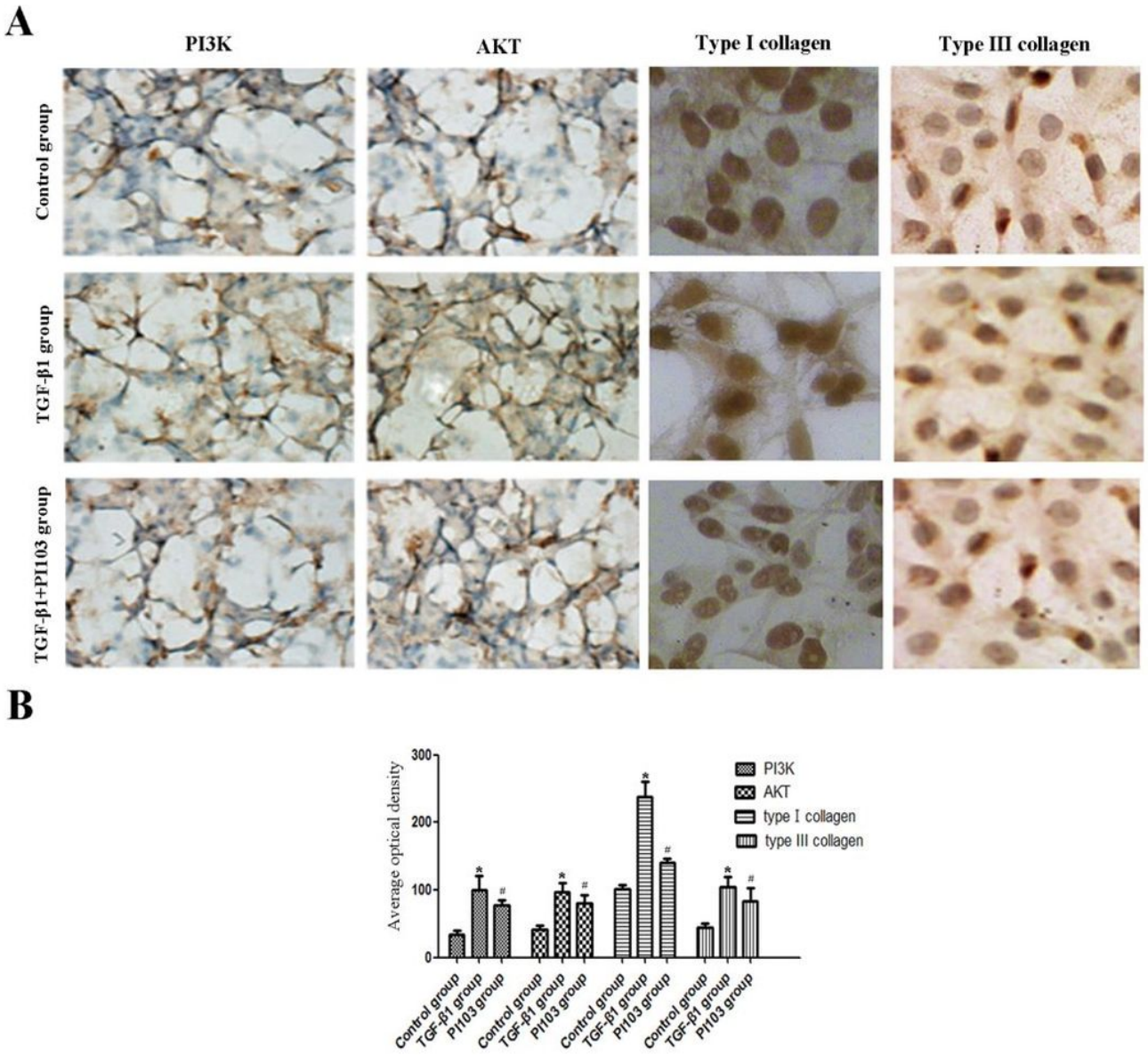

Figure 6

The protein expression was detected by immunocytochemistry method of hepatic stellate cells in different group (magnification, x200). **A** Immunocytochemistry graph. **B** The expressions of the average optical density of PI3K, Akt signal molecule and type Ⅰ, Ⅲ collagen in different groups. * represents $P<0.05$ compared to the control group; # represents $P<0.05$ compared with TGF-β1 group.

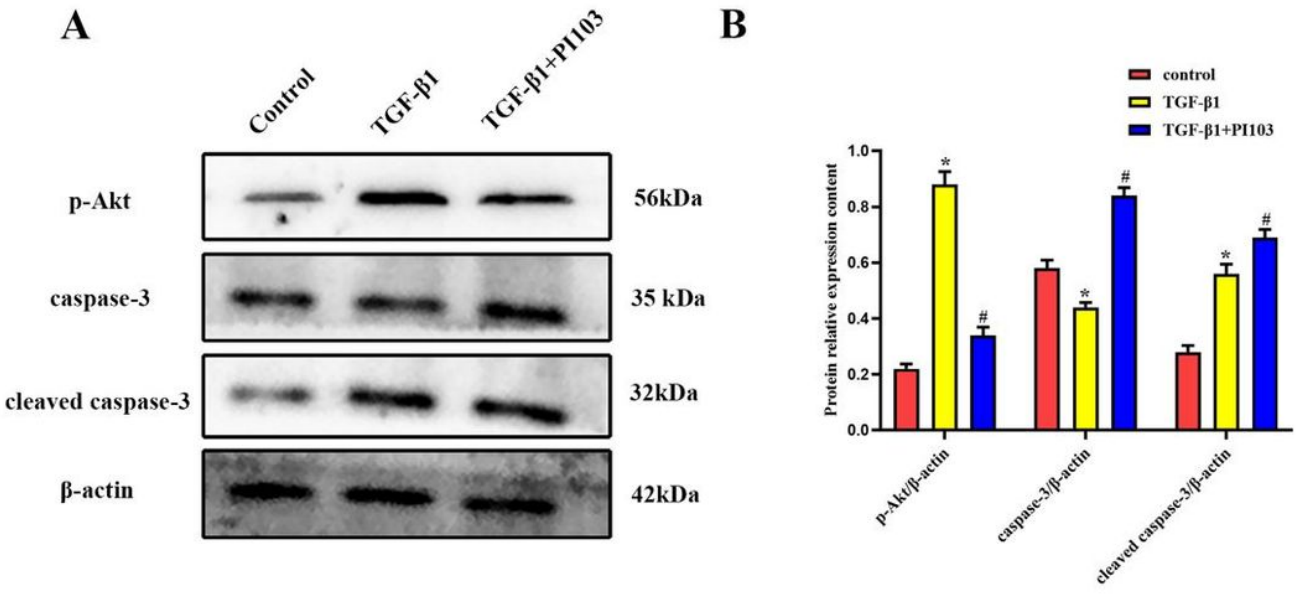

Figure 7

Changes in intracellular p-Akt, caspase-3 and cleaved caspase-3 protein levels. **A** The protein bands in HSC of p-Akt, caspase-3 and cleaved caspase-3. **B** Related proteins gray value analysis. * *P*<0.05 compared to the control group; # *P*<0.05 compared with TGF-β1 group.